Inter-Decadal Climate Variability in the Southern Hemisphere: Evidence from Tasmanian Tree Rings over the Past Three Millennia

Edward R. Cook, Brendan M. Buckley, and Rosanne D. D'Arrigo

ABSTRACT: The characterization of inter-decadal climate variability in the Southern Hemisphere is severely constrained by the shortness of the instrumental climate records. To help relieve this constraint, we have developed and analyzed a reconstruction of warm-season (November-April) temperatures from Tasmanian tree rings that now extends back to 800 BC. A detailed analysis of this reconstruction in the time and frequency domains indicates that much of the inter-decadal variability is principally confined to four frequency bands with mean periods of 31, 57, 77, and 200 years. These oscillations are stable and robust with respect to the progressive development and extension of the tree-ring reconstruction back in time. They account for about 12% of the overall variance in annual temperature estimates and 41% of the inter-decadal variance (*ie,* periods >10 years). Using singular spectrum analysis, we estimate the overall inter-decadal temperature signal contributed by these four oscillations and compare its recent behavior to an anomalous warming that has been in progress over Tasmania since about 1965. We find that 51% of the mean anomalous warming can be accounted for by these oscillations. Prediction error filtering is also used to forecast the inter-decadal temperature signal 30 years into the future. In so doing, we show how a future greenhouse warming signal over Tasmania could be masked by these natural oscillations unless they are taken into account.

Introduction

Characterization of inter-decadal climate variability worldwide is constrained by the shortness of the instrumental climate records. This problem is especially acute in the Southern Hemisphere, where such records rarely exceed 100 years in length (Barry 1978). In Tasmania, tree-ring width variations of old-growth Huon pines (*Lagarostrobos franklinii*) provide a means of extending instrumental temperature records back thousands of years. We analyze one such reconstruction of warm-season (November-April) temperatures for Tasmania, which now extends back to 800 BC. As will be shown, there is strong statistical evidence in the time and frequency domains for inter-decadal and century-scale variability of an oscillatory nature. This behavior is stable and robust with respect to the progressive development and extension of the tree-ring reconstruction back in time. Thus, we believe the oscillatory behavior in the series is not a statistical artifact. Rather, it reflects the true dynamics of the ocean/atmosphere system in this sector of the Southern Hemisphere.

In: C.M. Isaacs and V.L. Tharp, Editors. 1995. *Proceedings of the Eleventh Annual Pacific Climate (PACLIM) Workshop, April 19-22, 1994.* Interagency Ecological Program, Technical Report 40. California Department of Water Resources.

Tree-Ring Chronology Development

Tree-ring data used in the temperature reconstruction were collected from a disjunct stand of sub-alpine Huon pine at an elevation of 950 meters on Mount Read, in western Tasmania (Figure 1). The site is called "Lake Johnston" after a small cirque lake about 50-100 meters below the stand. The Huon pine stand is composed of two discrete, adjacent units: one made up solely of living trees and a second area of standing dead trees killed by a fire in 1961. All of the sub-fossil wood used to extend the reconstruction back in time came from the zone of fire-killed trees. Actual wood collections were made over a period of 4 years, with the living trees sampled first. This produced a tree-ring chronology spanning AD 779-1988 (Cook *et al* 1992). Subsequently, standing dead trees were sampled from the fire-killed zone, followed by remnant logs and stumps. The sub-fossil tree rings were exactly cross-dated in time with the living-tree chronology to extend the chronology back in time. Total overlap between the living tree and sub-fossil wood chronologies is 952 years.

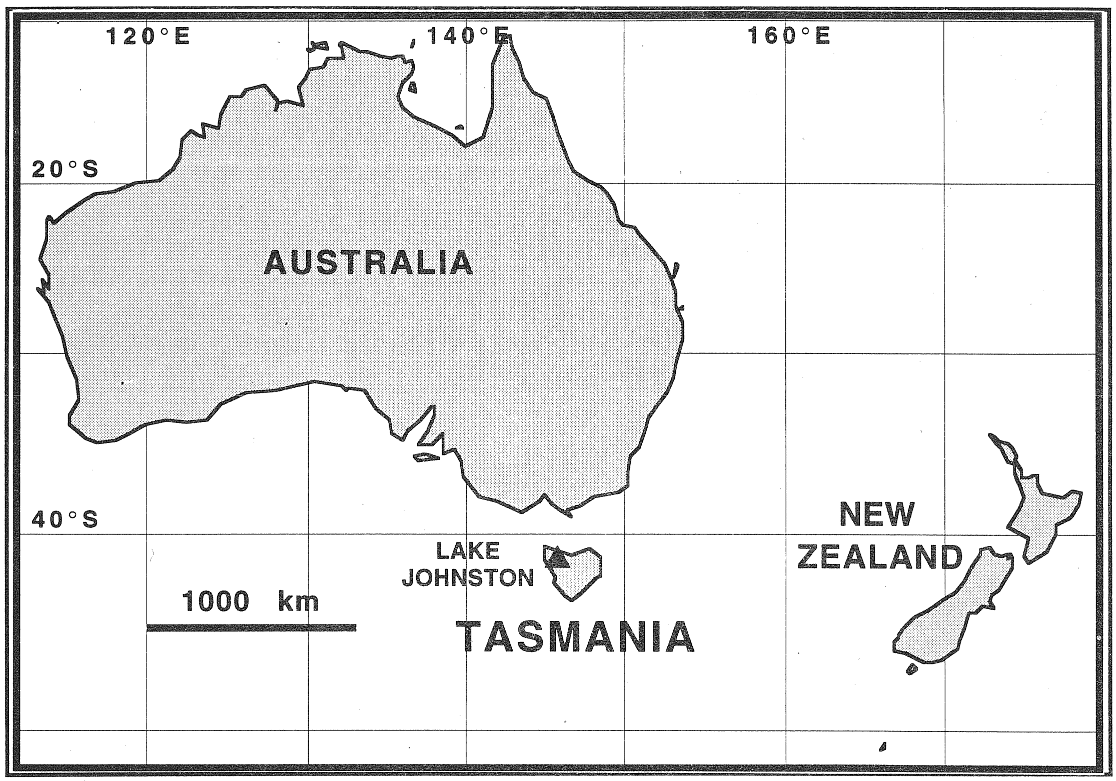

Figure 1. MAP SHOWING TASMANIA AND THE LAKE JOHNSTON TREE-RING SITE IN RELATION TO AUSTRALIA AND NEW ZEALAND

The raw tree-ring measurement series were standardized (Fritts 1976) using very conservative detrending to preserve as much low-frequency variance as possible in the data. In the newest, longest version of the chronology, which now extends back to 800 BC, only linear and negative exponential growth trends were removed from the individual segments. The final site chronologies thus produced for climatic reconstruction were mean-value functions of all cross-dated and standardized segments available at the time, averaged across years using the biweight robust mean to discount the influence of outliers.

Temperature Reconstructions

The warm-season temperature reconstruction analyzed here was developed in three discrete stages, representing the progressive addition of newly available tree-ring data to the reconstruction and the extension of that series farther back in time. These stages of development are shown in Figure 2. The first reconstruction covers AD 900-1989 and is described in Cook *et al* (1991, 1992). The second reconstruction covers 300 BC-AD 1989 and is described in Cook *et al* (in press). The third reconstruction, which will be analyzed here, covers 800 BC-AD 1991. So, in three independent stages, the length of the warm-season temperature reconstruction was increased from 1089 to 2290 and, finally, to 2792 years.

These progressive extensions also meant the addition of a lot of new tree-ring data throughout the record. Figure 2(d) shows the changing tree-ring sample size over time for each of the three reconstructions. From AD 900 to the present, most of the samples came from living trees. Prior to that date, the tree-ring specimens came from sub-fossil logs and *in situ* stumps at the site. Although the tree-ring samples added to the reconstruction are not spatially independent of those used initially by Cook *et al* (1991,1992) (*ie*, they all came from the same general location above Lake Johnston), they do represent many new trees sampled independently of the living trees.

Spectral analysis (Jenkins and Watts 1968; Marple 1987) of the three series in Figure 2 has revealed the presence of oscillatory behavior that has apparently persisted over the past 2792 years. Cook *et al* (1992) presented both classical Blackman-Tukey and maximum entropy spectra of the shortest record and noted the apparent presence of statistically significant (*a priori* $\alpha<0.05$) peaks with periods around 30, 56, 80, and 180 years. It was speculated that these peaks could have been generated by internal dynamics of the coupled atmosphere/ocean/cryosphere system (*sensu* Stocker and Mysak 1992). However, given the *a posteriori* nature of the spectral analysis, those results had to remain purely speculative. With the extension of the record back to 300 BC, which doubled the original series length, it was possible to test for the longer-term presence of those oscillatory modes and possibly validate their existence. In so doing, Cook *et al* (in press) found that the spectral peaks noted earlier were still present in the longer reconstruction, even when the series was split into two quasi-independent halves and analyzed separately. In this case, the mean periods for the full reconstruction were 31, 56, 79, and 204 years. With this positive result, Cook *et al* (in press) proceeded to characterize the time/domain behavior of these oscillations using singular spectrum analysis (Vautard and Ghil 1989). The extracted wave forms obtained by SSA revealed that these signals were indeed present throughout the reconstruction and possessed significant amplitude modulation. With the addition of more tree-ring series to the reconstruction and its extension back to 800 BC (Figure 2), we will again make the case for the probable existence of these oscillatory modes and characterize them using SSA.

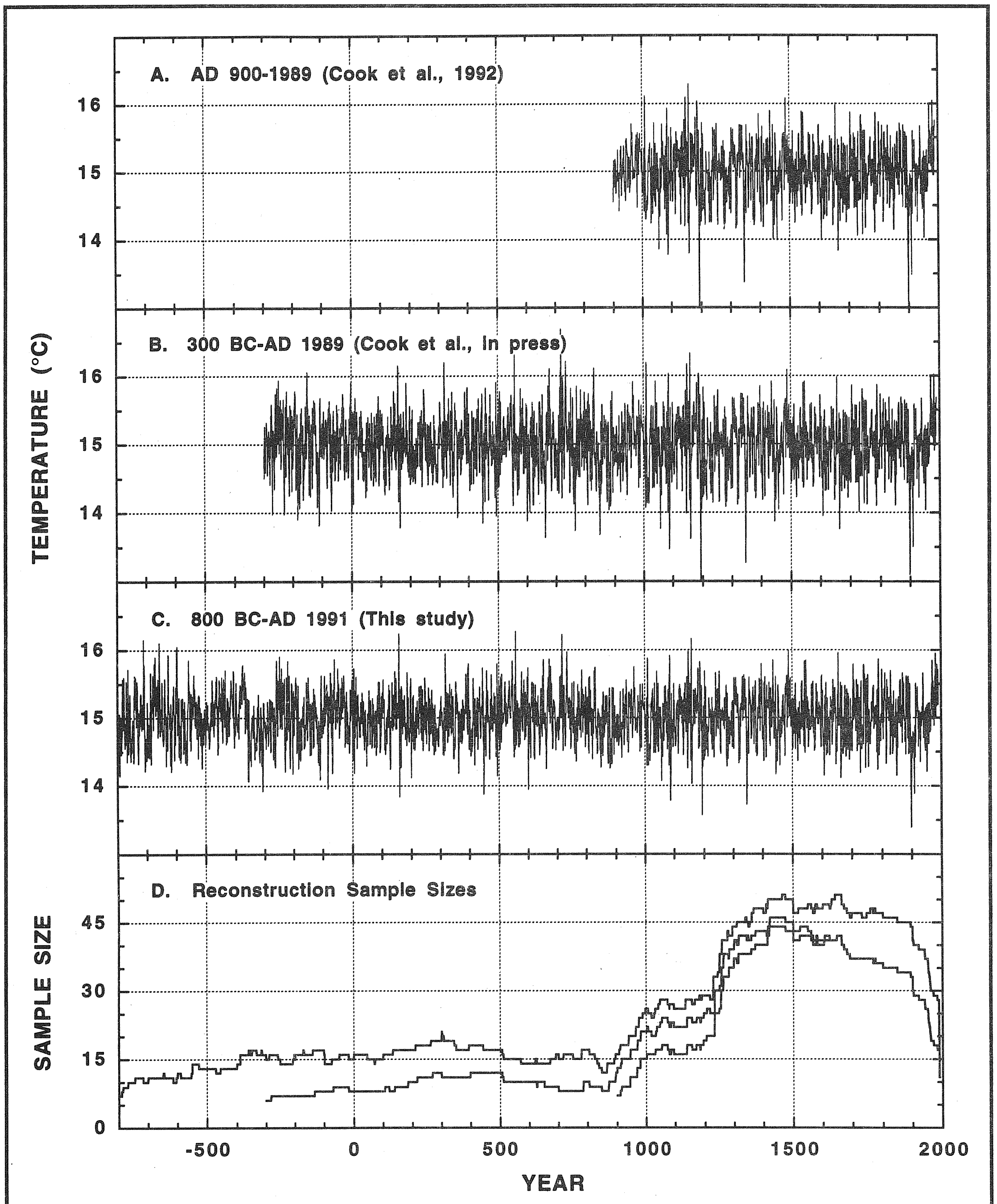

Figure 2. THREE TEMPERATURE RECONSTRUCTIONS USED TO DOCUMENT THE OSCILLATORY BEHAVIOR IN WARM-SEASON TASMANIAN TEMPERATURES
The change in tree-ring sample size is shown to indicate the degree to which new information was added to each successive reconstruction.

Figure 3 shows the power spectra of the three reconstructions developed to date. Each has been computed using identical Blackman-Tukey procedures. The spectral estimates are only shown over frequencies from 0 to 1/10 years, because that is the bandwidth of interest here. Relevant statistics of the power spectra are provided in the figure (*ie*, lags, degrees of freedom, bandwidth). The *a priori* 95% confidence limits are based on a first-order Markov null continuum model (Gilman *et al* 1963). It is arguable that the *a priori* limits are, in fact, correct for testing the spectra in Figure 3 (b-c) because the four spectral peaks being tested were known

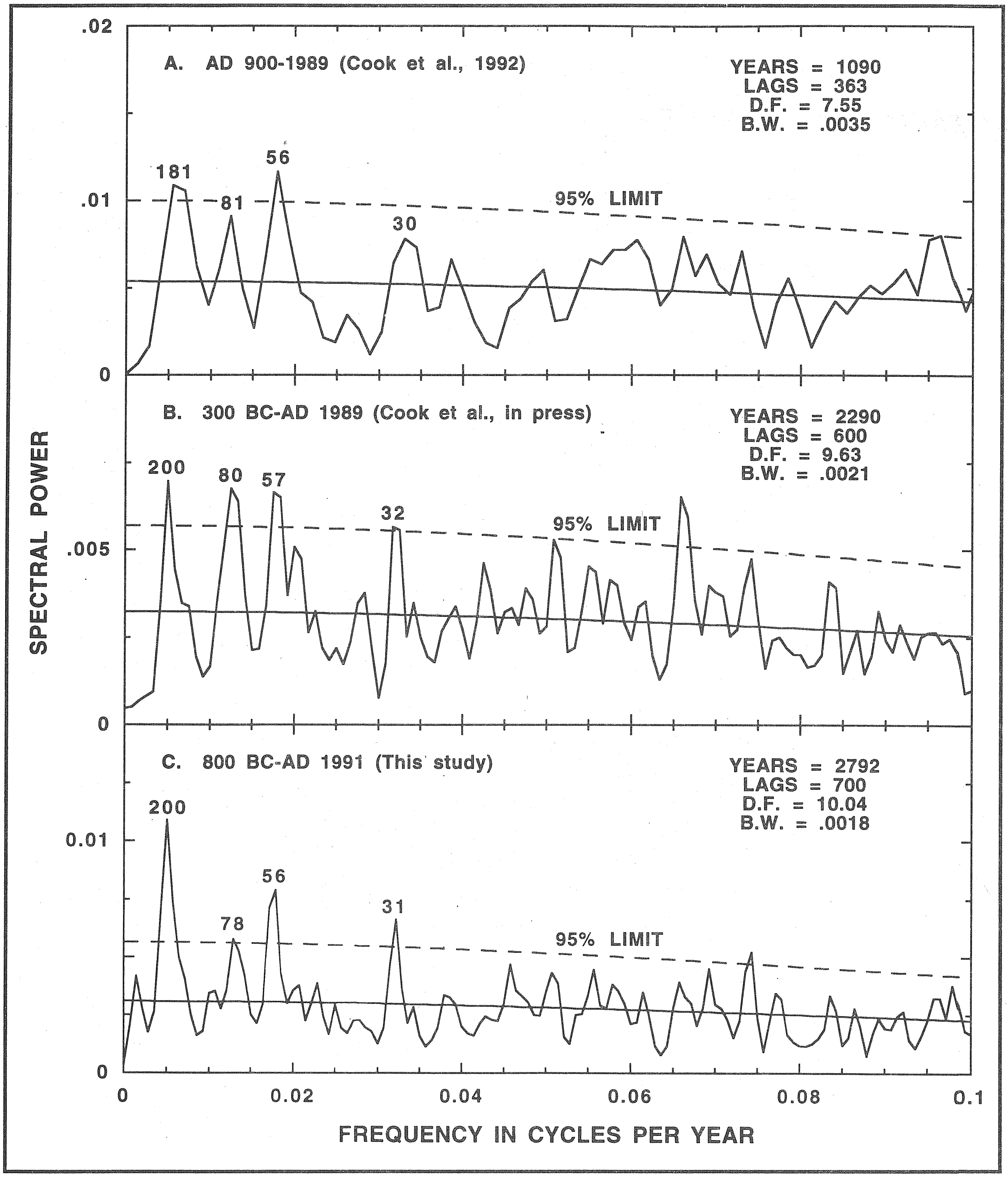

Figure 3. BLACKMAN-TUKEY POWER SPECTRA OF THE THREE RECONSTRUCTIONS SHOWN IN FIGURE 2.
The 95% confidence limits are based on a first-order Markov null continuum model.
The spectra are only shown over the frequency range 0 to 0.10.

in advance. However, the lack of complete independence of the times series analyzed here weakens that argument somewhat.

These spectra basically re-affirm the probable existence of the oscillatory modes reported by Cook *et al* (1992, in press). Each indicates the presence of spectral peaks with periods around 31, 56, 80, and 200 years, although their contributed variances do vary somewhat. In contrast, there is little indication of consistent spectral peaks in the frequency range of 1/28 to 1/10 years that exceed the 95% limits. This suggests that any indicated quasi-periodic behavior in that broad band is either transient or spurious.

Singular Spectrum Analysis

We now take a more detailed look at the oscillations in the Tasmania temperature reconstruction using SSA. The series used for this purpose is that shown in Figure 2(c), which extends back to 800 BC. Singular spectrum analysis is an elegant, data-adaptive method of extracting signals from noise in a time series (Vautard and Ghil 1989; Vautard *et al* 1992). It is based on applying principal components analysis to the autocovariance matrix of the time series. Following Vautard *et al* (1992), we used unbiased estimates of autocovariance for this purpose. The result is a set of eigenvalues (or "singular values") and eigenvectors (or "empirical orthogonal functions") that express particular modes of behavior in the series over time. In particular, periodic behavior is expressed in the eigenvalue trace as a degenerate pair of nearly equal eigenvalues. The corresponding EOFs will behave as even and odd functions, with the latter being in quadrature with the former. When applied to the original time series to extract the oscillatory wave form (or "reconstructed components"; Vautard *et al* 1992), the even and odd EOFs act as digital band-pass filters with data-derived frequency response functions. This is one of the principal strengths of singular spectrum analysis, because it does not impose a potentially incorrect band-limited model on the series as might be the case using classical digital filtering techniques. On the other hand, the reconstructed components produced by SSA might not be physically interpretable beyond a phenomenological level and could, in fact, be transient or totally spurious. The oscillations being investigated here do not appear to be either transient or spurious. However, their physical meanings are still somewhat elusive.

Like all methods of spectral analysis, there is an element of subjectivity and even artwork in applying singular spectrum analysis to noisy time series. Two matters are of particular interest. One is determining the dimension of the signal subspace; *ie*, the number of "true" signals in the time series. Given the link between singular spectrum analysis and principal components analysis, this is equivalent to determining the number of significant eigenvalues in the autocovariance matrix. Monte carlo techniques could be used for this purpose using one of the methods described in Preisendorfer *et al* (1981) if nothing is known about the signal subspace dimension. Such is not the case here. A related problem, which does not normally exist in PCA, is selecting the optimum embedding dimension for extracting the signals of interest; *ie*, the number of lags used to estimate the autocovariance matrix. Here, the link between SSA and classical Blackman-Tukey spectral analysis is apparent, because the chosen lag window ultimately determines the resolution and stability of spectral estimates in either case.

In our problem here, the number of "true" signals has been defined by previous analyses (Cook *et al* 1992; in press). This means we should expect four pairs of eigenvalues to express the oscillatory behavior associated with the 31-, 56-, 80-, and 200-year modes. In addition, these four periodic components consistently account for most of the band-limited variance in the spectrum at wave-lengths longer than 10 years. Thus, they should be associated with the first eight eigenvalues of the autocovariance matrix if the analysis is restricted to inter-decadal or longer wave-lengths. This is the expected dimension of our signal subspace. The choice of embedding dimension can have an effect on this expectation, however. If it is too small, there will not be sufficient resolution to cleanly separate the oscillatory modes into separate EOF pairs. In this case, the variance associated with the four modes may be condensed into fewer than eight eigenvalues. Conversely, too many lags can lead to something akin to peak splitting, which may cause the variance to be distributed over more than eight eigenvalues.

Because there is no theory for determining the optimum embedding dimension, a form of "window closing" (*sensu* Jenkins and Watts 1968) is usually applied in SSA to search for a range of embedding dimensions where the results do not change very much (Vautard and Ghil 1989; Vautard *et al* 1992). We have used this window closing procedure here, but have adapted it to the individual oscillations, which range from 31 to 200 years. In each case, five embedding dimensions *(M)* were investigated. For the 200-year oscillation, *M* ranged from 300-500 at 50-lag intervals. For the closely spaced 56- and 80-year oscillations, *M* ranged from 200-400 also at 50-lag intervals. For the 31-year oscillation, *M* ranged from 100-200 at 25 lag intervals. Prior to each window closing exercise, we filtered the temperature reconstruction to eliminate higher-frequency variance not associated with the oscillations being modeled. Pre-filtering eliminated some leakage problems apparent in the EOFs, which would have degraded their performance as band-pass filters. However, the EOFs estimated after pre-filtering were always applied to the original, unfiltered reconstruction when estimating the reconstructed components.

Figure 4 shows the reconstructed components using the procedures described above. Component periods were determined by spectral analysis and differ only slightly from the earlier estimates (77 *vs* 80 and 57 *vs* 56 years). Rather than present one reconstructed component per oscillation as the "best" estimate, we have chosen to overlay all five in each case for comparison. In general, the estimated reconstructed components are not sensitive to the choice of embedding dimension. The biggest differences tend to be during periods of reduced amplitude; *ie,* when the signal-to-noise ratio was lowest. In every case, the reconstructed components show distinct amplitude modulation with a typical range of near zero to 0.1°C. In some cases, the modulation envelope is somewhat regular, the 77-year reconstructed component being the best example. The 31-year reconstructed component also has a tendency for asymmetric, non-linear amplitude modulation, with the rise taking longer than the fall.

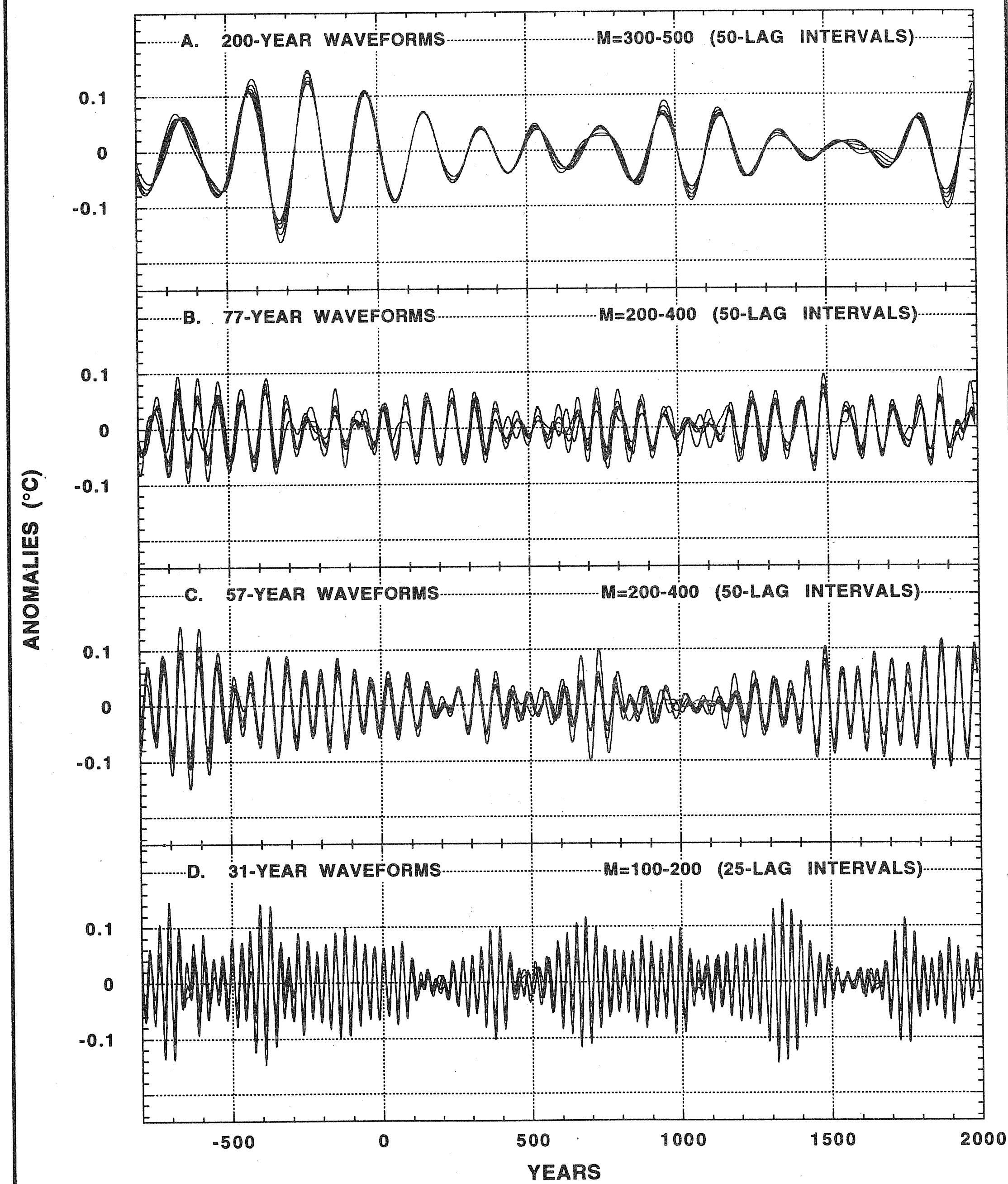

Figure 4. WAVEFORMS OF THE TEMPERATURE OSCILLATIONS EXTRACTED BY SINGULAR SPECTRUM ANALYSIS
Five waveforms per period were estimated and overlaid to indicate the degree to which the chosen embedding dimension affected results.

There is no obvious "best" embedding dimension for selecting the 31-, 57-, 77-, and 200-year reconstructed components to produce a composite temperature signal that expresses the cumulative effect of these inter-decadal oscillations through time. For this reason, we generated all possible combinations of 4-wave form aggregates using the five estimates per oscillation. This resulted in 5^4 or 625 aggregates. We then took the median aggregate as the best estimate of the inter-decadal temperature signal based on the four oscillations. In addition, we used the 2.5 and 97.5 percentiles of the 625 aggregates to generate approximate 95% confidence limits around the median series. These results are shown in Figure 5. From these plots, it is clear that the variance due to the choice of embedding dimensions is quite small relative to the amplitude of the median signal.

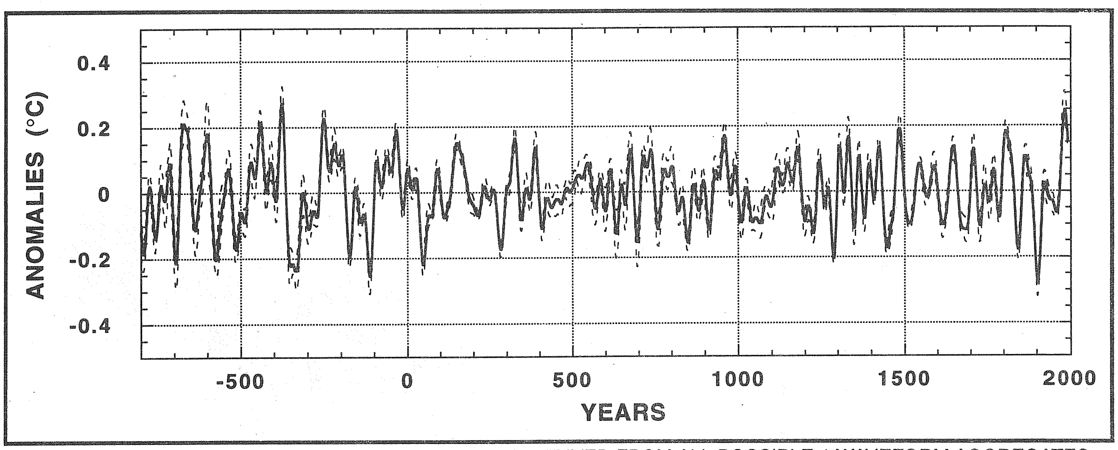

Figure 5. MEDIAN AGGREGATE WAVEFORM (solid curve) DERIVED FROM ALL POSSIBLE 4-WAVEFORM AGGREGATES AVAILABLE FROM FIGURE 4.
The 2.5 and 97.5 percentile limits (dashed curves) from the suite of all possible aggregates are provided as approximate 95% confidence limits.

None of individual oscillations accounts for more than 2 or 3% of the total variance in the original temperature reconstruction, but individual oscillations are much more important when viewed in the context of inter-decadal climate variability alone. Figure 6 shows scatter plots of the median aggregate signal versus the original unfiltered reconstruction and the series after being low-pass filtered to eliminate all variance at periods less than 10 years. The median aggregate has a correlation of 0.35 with the original series; *ie,* it accounts for 12% of the total variance. In contrast, the correlation with the low-pass-filtered series is 0.64, which amounts to 41% of the inter-decadal variance. Thus, in the context of inter-decadal climate variability over Tasmania, these oscillations must be considered highly important contributors.

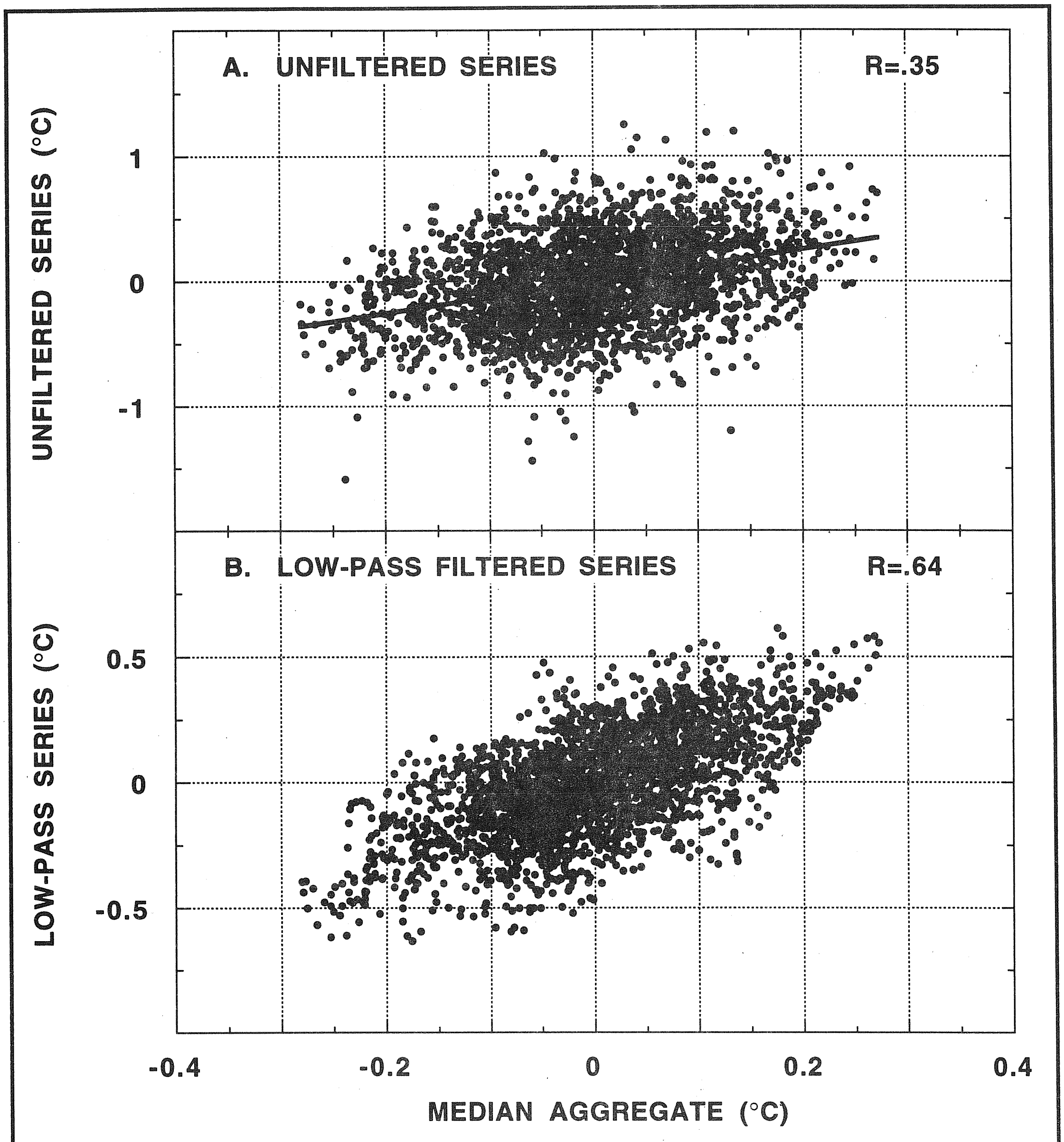

Figure 6. SCATTERPLOTS OF THE MEDIATE AGGREGATE VERSUS THE UNFILTERED AND LOW-PASS FILTERED TEMPERATURE RECONSTRUCTIONS.
Correlations are indicated in the upper righthand corners of the plots.

Temperature Oscillations and Recent Warming over Tasmania

It is instructive now to see how much these oscillations have contributed to recent anomalous warming over Tasmania that was documented by Cook *et al* (1991, 1992). In the AD 900-1989 reconstruction, the 1965-1989 interval was found to be the warmest 25-year period in the 1089-year record. Only when the reconstruction was extended back more than 2000 years was a warmer 25-year period found. In the longest reconstruction, the two warmest 25-year periods are 387-363 BC (0.35±0.046°C) and 1967-1991 (0.33±0.055°C). So while not unique, the most recent warming is still a rare event that exceeds the long-term mean by 6 standard errors.

With regard to the temperature oscillations being studied here, an obvious question is: "Can they explain the recent warming over Tasmania?" If not, then it could be argued that the climate system is in a new, radiatively altered state due to the buildup of greenhouse gases in the 20th century. Returning to Figure 5, it appears that the oscillations can explain much of the anomalous temperature variability seen in the original reconstruction. The two warmest periods in the median aggregate are the same as before, with peak anomalies of 0.27°C in 376 BC and 0.25°C in 1982.

Figure 7 shows the outer portion of this temperature signal with its 95% limits superimposed on the low-pass filtered reconstruction. The latter highlights the general inter-decadal temperature fluctuations, including the recent warming. For ease of examination, these series are only shown since 1800. It is clear from these plots that the temperature oscillations can cumulatively explain a large fraction of the overall warming since 1967. In terms of mean anomalies, the low-pass-filtered series averages 0.35±0.015°C for 1967-1991, while the mean of the median aggregate is 0.18±0.014°C. So, about 51% of the anomalous warmth can be attributed to the temperature oscillations. This occurred because the individual oscillation anomalies were relatively large, positive, and in phase at this time by chance. However, this comparison may be slightly biased because the 1967-1991 period was used in estimating the EOFs, making the comparison in Figure 7 analogous to results of a fitting exercise. If these data were not used, it is possible that the resulting EOFs would not produce reconstructed components that predict the warming as well. This possibility will be investigated, but it is unlikely to make a large difference. Even withholding all of the 20th century data from estimates of the autocovariances and EOFs would only amount to reducing the series by 3.3% of its total length.

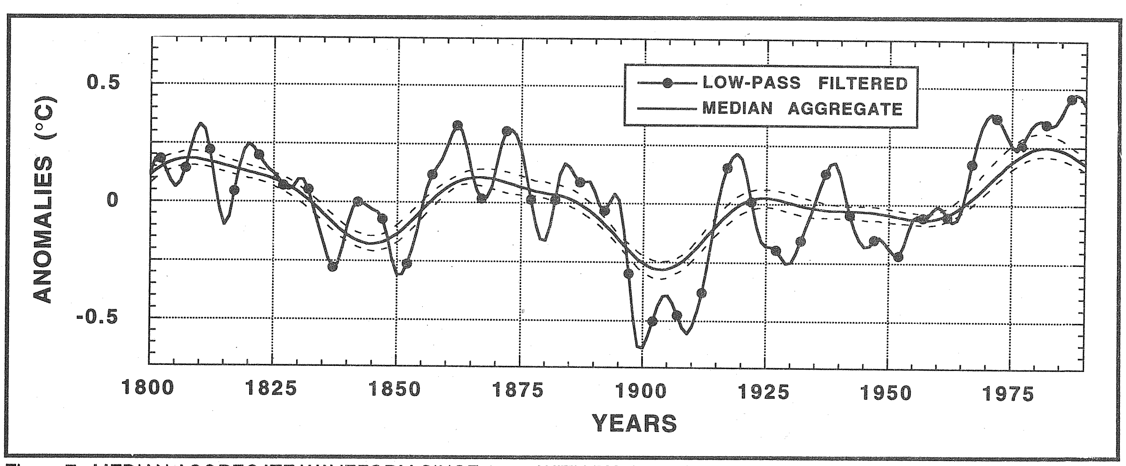

Figure 7. MEDIAN AGGREGATE WAVEFORM SINCE 1800, WITH ITS APPROXIMATE 95% CONFIDENCE LIMITS COMPARED TO THE LOW-PASS FILTERED SERIES

Note the degree to which the aggregate explains much of the inter-decadal warming in the reconstruction since 1965.

Given that the oscillations apparently explain over half of the mean anomalous warming, the median aggregate still systematically underestimates the magnitude of change indicated by the inter-decadal fluctuations. While it is tempting to speculate that greenhouse forcing could be responsible for this residual anomalous warming, systematic under- and over-estimates of inter-decadal temperature change by the median aggregate are as large or larger for similar duration periods in the past. Clearly, there are additional contributors to inter-decadal temperature change over Tasmania, but none seem to be as systematically and persistently effective over the past three millennia as those investigated here.

Implications for Detecting a Greenhouse Warming

The inter-decadal temperature oscillations over Tasmania have the potential to either mimic or mask expected temperature trends due to greenhouse warming. This potential is clearly indicated in Figure 7, where the oscillations collectively explain 51% of the recent anomalous warming. Yet, a closer examination of the median aggregate indicates that it may now be on a down-turn, while the overall inter-decadal temperature trend is stable or rising slightly. Does this mean a divergence is underway that could be reflecting the emergence of greenhouse warming from the natural background variability? It is impossible to say at this time. However, it is possible to describe a reasonable scenario in which the masking effect of the oscillatory modes is factored from expectations of a hypothetical future temperature regime to reveal anomalous warming.

Consider the scenario in which the temperature increase over Tasmania occurred as an abrupt change of state. This is plausible, given the rather rapid and persistent temperature increase that occurred shortly after 1965 in both the instrumental record and the reconstruction (Cook *et al* 1992). Next, suppose this change of state is maintained for the next 30 years (*ie,* no further warming occurs), while at the same time the inter-decadal oscillations continue to operate as they have for the last three millennia. A stable mean maintained over the next 30 years would seem to argue against greenhouse forcing because a warming trend is the first-order (albeit non-unique) expectation, at least on a hemispheric basis. However, maintaining a stable mean would actually require a warming trend from other sources, like greenhouse forcing, to offset a continuing decline by the oscillations in the future.

To see how this might work, the median aggregate was forecast 30 years into the future using a moderate-length prediction error filter estimated by the maximum entropy method (Ulrych and Clayton 1976). The resulting inter-decadal 30-year forecast is shown in Figure 8, along with a simple climatology forecast based on the 1967-1991 mean. The inter-decadal forecast is not sensitive to the prediction error filter length. Varying the order from 200 to 500 produced almost no difference in the forecasts. This is due to the extremely high signal-to-noise ratio in the median aggregate produced by singular spectrum analysis (cf, Penland *et al* 1991) and the short forecast horizon relative to the lengths of the prediction error filters tested.

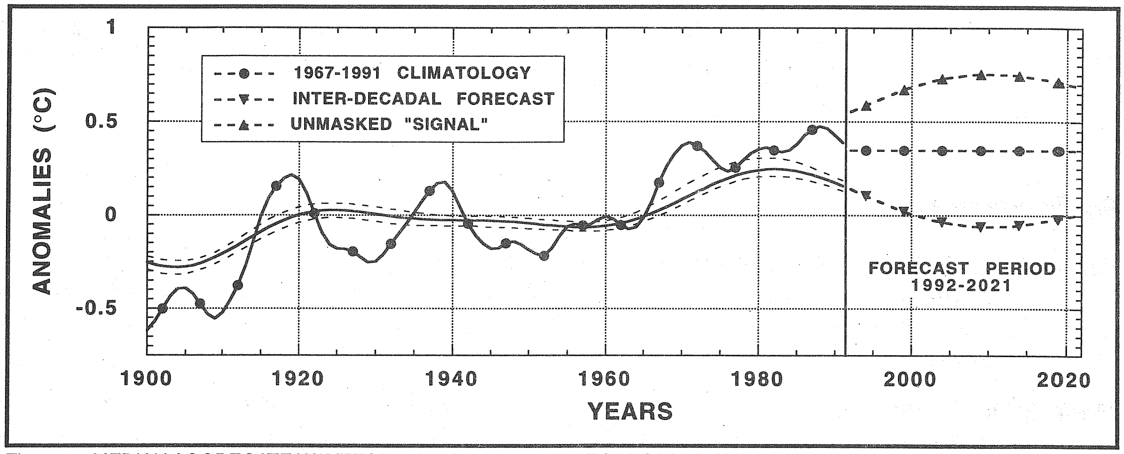

Figure 8. MEDIAN AGGREGATE WAVEFORM SINCE 1900, WITH FORECASTS OUT TO THE YEAR 2021
These are provided to indicate how such inter-decadal, natural variability could mask a future warming trend due to other effects like greenhouse warming. This forecast is compared to a climatology forecast using the mean of the 1967-1991 period, which represents a continuation of the anomalous warmth now affecting Tasmania. If both were to occur in the future, a hidden warming trend indicated by the unmasked "signal" would be required to offset the inter-decadal cooling.

As suspected, the inter-decadal forecast continues to decline from its recent peak in 1982 to a minimum in 2009, after which it begins to climb slowly again. The unmasked hypothetical change is that needed to completely offset the inter-decadal cooling and thus reproduce the climatology forecast. Therefore, it is nothing more than the mirror image of the inter-decadal cooling. The result is an unmasked warming trend. In its unmasked state, this trend would exceed the warmest 25-year period in the reconstruction by a wide margin over the next 30 years. Although rather schematic and strictly hypothetical, this example illustrates how future warming induced by factors not related to the inter-decadal oscillations would have to be substantial just to offset a projected cooling due to this long-term, natural variability.

Conclusions

We have presented a growing body of statistical evidence for the existence of inter-decadal temperature oscillations affecting the climate of Tasmania. This behavior has apparently persisted for almost 3000 years and is an important contributor to past and present temperature change in this sector of the Southern Hemisphere. Although it is always dangerous to extrapolate such results into the future, it is reasonable to expect that these oscillations will continue in more or less the same modes unless a radical change of state occurs in the ocean/atmosphere system. If this behavior continues, then the potential masking effects of these oscillations on a greenhouse warming will need to be considered.

Acknowledgments

We thank Trevor Bird, Mike Peterson, Roger Francey, and Mike Barbetti for field assistance and valuable consultations on Huon pine research in Tasmania. This research is supported by the National Science Foundation, Division of Earth Sciences (Grant EAR 93-10093) and Division of Atmospheric Sciences (Grant ATM 92-12107).

References

Barry, R.G. 1978. Climatic fluctuations during the periods of historical and instrumental record. Pages 150-166 in *Climatic Change and Variability: A Southern Hemisphere Perspective*. A.B. Pittock, L.A. Frakes, D. Jenssen, J.A. Peterson, J.W. Zillman, editors. Cambridge University Press, London.

Cook, E.R., T. Bird, M. Peterson, M. Barbetti, B. Buckley, R. D'Arrigo, R. Francey, P. Tans. 1991. Climatic change in Tasmania inferred from a 1089-year tree-ring chronology of subalpine Huon pine. *Science* 253:1266-1268.

Cook, E.R., T. Bird, M. Peterson, M. Barbetti, B. Buckley, R. D'Arrigo, R. Francey. 1992. Climatic change over the last millennium in Tasmania reconstructed from tree rings. *The Holocene* 2:205-217.

Cook, E.R., B.M. Buckley, R.D. D'Arrigo. In press. Interdecadal temperature oscillations in the southern hemisphere: Evidence from Tasmanian tree rings since 300 BC. In *The Natural Variability of the Climate System on 10-100 Year Time-Scales*. Proceedings of National Academy of Sciences Workshop, Irvine, California, September 21-24, 1992.

Fritts, H.C. 1976. *Tree Rings and Climate*. Academic Press, London.

Gilman, D.L., F.J. Fuglister, and J.M. Mitchell Jr. 1963. On the power spectrum of "red noise". *Journal of the Atmospheric Sciences* 20:182-184.

Jenkins, G.M., and D.G. Watts. 1968. *Spectral Analysis and Its Applications*. Holden-Day, San Francisco.

Marple, S.L. Jr. 1987. *Digital Spectral Analysis with Applications*. Prentice-Hall, New Jersey.

Penland, C., M. Ghil, K.M. Weickmann. 1991. Adaptive filtering and maximum entropy spectra with application to changes in atmospheric angular momentum. *Journal of Geophyiscal Research* 96(D12):22,659-22,671.

Preisendorfer, R.W., F.W. Zwiers, T.P. Barnett. 1981. *Foundations of Principal Components Selection Rules*. SIO Reference Series 81-4, Scripps Institution of Oceanography, La Jolla.

Stocker, T.F., and L.A. Mysak. 1992. Climatic fluctuations on the century time scale: A review of high-resolution proxy data and possible mechanisms. *Climatic Change* 20:227-250.

Ulrych, T.J., and R.W. Clayton. 1976. Time series modeling and maximum entropy. *Physics of the Earth and Planetary Interiors* 12:188-200.

Vautard, R., and M. Ghil. 1989. Singular spectrum analysis in nonlinear dynamics, with applications to paleoclimatic time series. *Physica D* 35:395-424.

Vautard, R., P. Yiou, M. Ghil. 1992. Singular spectrum analysis: A tool kit for short noisy chaotic time series. *Physica D* 58:95-126.